Direct Measurement of Lorentz Forces
in an Applied-Field MPD Thruster

IEPC-2005-65

H. Tobari[*], A. Ando[†], M. Inutake[‡] and K. Hattori[§]

Department of Electrical Engineering, Graduate School of Engineering, Tohoku University,
6-6-05, Aoba-yama, Sendai, 980-8759, Japan

Abstract: **In order to clarify flow and electromagnetic characteristics of an applied-field magneto-plasma-dynamic thruster (MPDT), spatial profiles of flow field and magnetic field near the outlet of the MPDT are measured and Lorentz force acting in the plasma is evaluated. It was found for the first time that the radial component F_r is dominant among three components of the Lorentz force, while the axial one F_z is much smaller than F_r in the measured region. An axial acceleration force is weakened by a deceleration force, which spontaneously appeared in an applied-field MPDT due to a diamagnetic effect of a high-beta plasma. The deceleration force can be converted to the acceleration one in an externally-applied diverging magnetic field.**

Nomenclature

I_d	=	discharge current
V_d	=	discharge voltage
e	=	charge of an electron
p	=	plasma pressure
m	=	mass of a particle
n	=	number density of a species
dm/dt =		mass flow rate of working gas
u	=	plasma flow velocity
E	=	electric field in plasma
B	=	magnetic field in plasma
B_0	=	externally applied magnetic field
j	=	plasma current density
F	=	Lorentz force per unit volume
k_B	=	Boltzmann's constant
T	=	particle temperature

[*] Research associate, Department of Electrical Engineering, tobari@ecei.tohoku.ac.jp
[†] Associate professor, Department of Electrical Engineering, akira@ecei.tohoku.ac.jp
[‡] Professor, Department of Electrical Engineering, inutake@ecei.tohoku.ac.jp
[§] Research associate, Department of Electrical Engineering, hattori@ecei.tohoku.ac.jp

I. Introduction

ELECTRIC propulsion is one of the promising space propulsion methods because of its high specific impulse which is unattainable by conventional chemical and nuclear propulsion[1]. A magneto-plasma-dynamic thruster (MPDT), which has coaxial electrodes consisting of a central cathode rod and an annular anode, has been developed as one of a high enthalpy plasma source with a high-specific impulse for space mission targeting from orbital maneuver to interplanetary transportation. Propellant gas is provided in the upstream region of the flow channel and is ionized by an arc discharge. If the arc current is high enough (more than about 1kA), a plasma is expected to be accelerated directly by an axial Lorentz force $j_r \times B_\theta$, where j_r is radial discharge current and B_θ is self-induced azimuthal magnetic field. In order to enhance the acceleration performance of the MPDT, it has been proposed to operate in various types of an externally-applied axial magnetic field B_0. In this case, in addition to the axial acceleration, the interaction between j_r and B_0 generates an azimuthal acceleration force, which drives the plasma to rotate azimuthally. Conversion of rotational momentum into axial momentum enhances plasma acceleration by passing through a magnetic nozzle. Further, an additional axial acceleration is expected by the interaction between azimuthally-induced Hall current j_θ and a radial magnetic field B_r under appropriate operating conditions (Hall acceleration and magnetic nozzle acceleration). Additionally, it is noted that plasma rotation by applying B_0 reduces a concentration of discharge current on the electrodes and is effective for preventing electrode erosion.

In previous experimental works[2-4], the MPDT were attempted to operate with the external magnetic field applied by a simple solenoid coil or permanent magnet and an increase in the thrust were measured actually. However, mechanisms of the increase in the thrust have not been clarified enough experimentally or theoretically. Though it is essential to clarify the acceleration mechanism for an MPDT plasma, there has been made no precise observation of a flow field and electromagnetic force (Lorentz force) field working on the plasma.

In this paper, we report experimental results of flow field and Lorentz force field measured near the outlet region of an applied-field MPDT. Formulas for the rotational phenomena of the applied-field of MPDT plasma are presented and Lorentz force field is evaluated from direct measurement of the magnetic field near MPDT muzzle.

II. Experimental apparatus

Experiments are performed in the HITOP (HIgh density TOhoku Plasma) device of Tohoku university[5-7]. The HITOP device consists of a large cylindrical vacuum chamber (diameter $D = 0.8$ m, length $L = 3.3$ m) and external magnetic coils, which can generate a uniform magnetic field up to 1kG, as shown in Fig.1. Various types of magnetic field configurations can be formed by adjusting these coil currents. A high-power, quasi-steady MPDT installed at one end of the HITOP device has a coaxial structure with a center tungsten rod cathode (10 mm in outer diameter) and an annular molybdenum anode (30 mm in inner diameter). A side view of the MPDT is shown in Fig. 2. The position of $Z=0$ is at the tip of the MPDT cathode. A quasi-steady discharge continues for 1 msec with a pulse-forming-network (PFN) and a fast acting gas valve puffs working gas into the discharge region. Discharge current I_d can be controlled by varying the charging voltage of the PFN power supply. Maximum value of I_d is 10 kA and a typical discharge voltage V_d is 200 V.

A spectroscopic method is used for measurements of ion temperature T_i, axial and azimuthal (rotational) flow velocities u_z, u_θ in the outlet region of the MPDT. The ion temperature and flow velocities are obtained from Doppler broadening and spectral shift of line spectra, which are detected with an image intensifier tube coupled with a CCD camera set at the exit plane of a Czerny-Turner spectrometer with a focal length of 1 m and a grating 2400 grooves/mm. In case of helium as the working gas, HeII line ($\lambda = 468.58$ nm) is detected to measure T_i, u_z and u_θ.
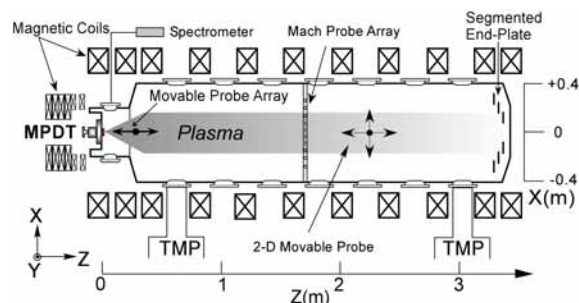
Figure 1. Schematic view of the HITOP device.
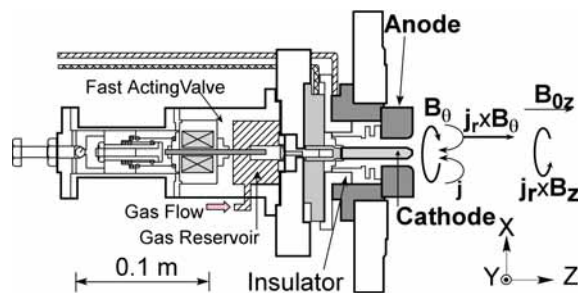
Figure 2.   A side view of the MPD thruster.

Time-varying magnetic fields in the plasma flow are measured directly by use of a movable magnetic probe array, which consists of 11 magnetic probes arrayed in the radial direction. Plasma current density can be calculated with the magnetic field data. Each probe has three sets of mutually perpendicular pick up coils to measure three components of the magnetic field variation ΔB_r, ΔB_θ and ΔB_z. Probe signals (*B*-dot signals) are transferred to differential amplifiers and integrators and digitized with 1M samples per second.

III.   Experimental results

A. Plasma rotation in an axial magnetic field

Characteristics of a plasma flow near the outlet of an applied-field MPDT are investigated spectroscopically. Figure 3 shows radial profiles of u_θ in a uniform magnetic field B_0 of 870 G and 500 G with helium mass flow rate dm/dt of 0.1g/s. The u_θ increases both with an increase in B_0 and linearly with the radius up to the inner radius of the anode (core region), that is, angular frequency ω keeps constant in the core region. This indicates the plasma column rotates as a rigid body. Plasma rotational energy is one of key parameters for clarifying acceleration mechanisms. Therefore we make an attempt to formulate the equilibrium of rotational plasma column near the outlet of the MPDT.[5]

A radial component of equation of motion is

$$m_i n_i \left(u_\theta^2 / r \right) - \left(\partial p / \partial r \right) + j_\theta B_z - j_z B_\theta = 0 \tag{1}$$

where p is plasma pressure rewritten as $p = p_i + p_e = k_B(n_i T_i + n_e T_e)$. A radial component of Generalized Ohm's law is written as,

$$e n_i \left(E_r + u_\theta B_z - u_z B_\theta \right) - \left(j_\theta B_z - j_z B_\theta \right) + \partial p_e / \partial r = 0 \tag{2}$$

From two equations, u_θ is expressed as follows,

$$u_\theta = -\frac{E_r}{B_z} + u_z \frac{B_\theta}{B_z} - \frac{m_i u_\theta^2}{e r B_z} + \frac{k_B T_i}{e} \frac{\partial \ln n_i}{\partial r} \tag{3}$$

Each term of the right hand side corresponds to $E \times B$ drift, effect of a helical stream line attributed to the helical magnetic field, a centrifugal force drift and an ion diamagnetic drift, respectively. Since measured emission intensity profile is Gaussian, ion density profile is assumed to be also Gaussian, that is, $n_i(r) = n_0 \exp(-r/r_0)^2$. Then E_r from Eq.(3) is expressed as follows,

$$E_r = -\frac{2r}{r_0^2} \frac{k_B T_i}{e} - \frac{m_i u_\theta^2}{re} - \left(u_\theta B_z - u_z B_\theta \right) \tag{4}$$
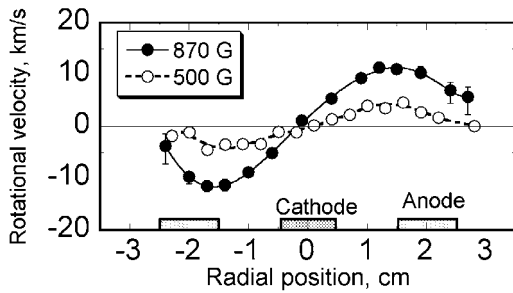
Figure 3. Radial profile of rotational velocity. I_d = 7.2 kA, Z = 9cm, B_0 = 870 G (solid circles) and 500 G (open circles).
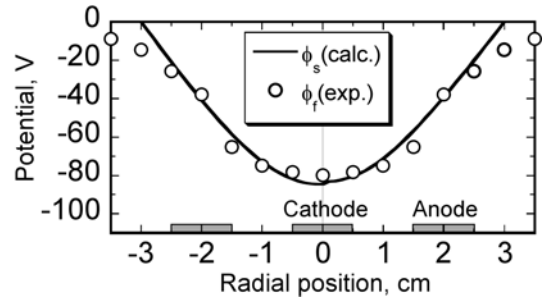
Figure 4. Comparison between radial profiles of calculated plasma potential (solid line) and measured floating potential (open circles).

3

Plasma potential can be calculated from a radial profile of E_r mentioned above. Figure 4 shows a comparison between the calculated plasma potential and the measured floating potential near the outlet of the MPDT in B_0 of 870 G. Note that the space potential is calculated as fixing $\phi_s = 0$ V at X = ±3 cm and the floating potential is measured by a Langmuir probe at Z = 9 cm. Both of the potential profiles are parabolic and they are in good agreement with each other.

These results indicate that the plasma rotation is not determined only by $E \times B$ drift. Although the direction of plasma rotation corresponds to that of $E \times B$ drift, the dependence of u_θ on the applied-field intensity contradicts with E_r / B_z. The plasma column rotates azimuthally as a result of a balance among the $E \times B$ drift, the effect of a helical stream line, the centrifugal force drift and the ion diamagnetic drift. When the applied-field strength increases, the on-axis plasma potential drops and the radial electric field increases, so that the $E \times B$ drift is enhanced. Also the plasma density increases with the increase of the applied-field, resulting that the diamagnetic drift becomes large, the direction of which is opposite to that of the $E \times B$ drift. It is found that the applied-field MPDT plasma rotates as a rigid body due to these drift terms.
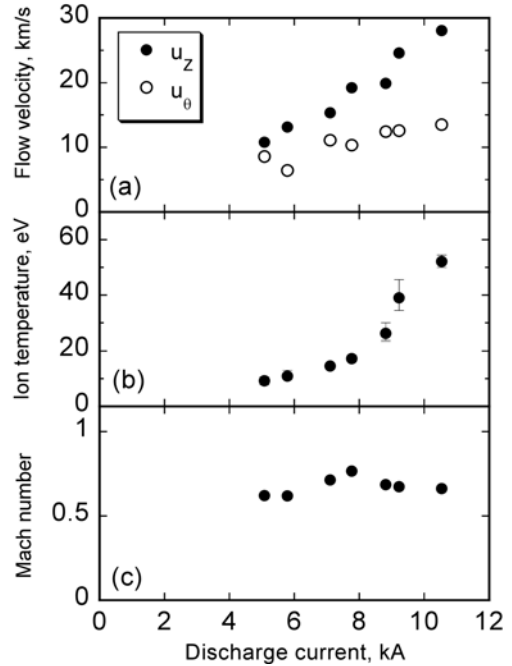
Figure 5. Dependence of (a) flow velocity, (b) ion temperature and (c) ion acoustic Mach number on the discharge current.
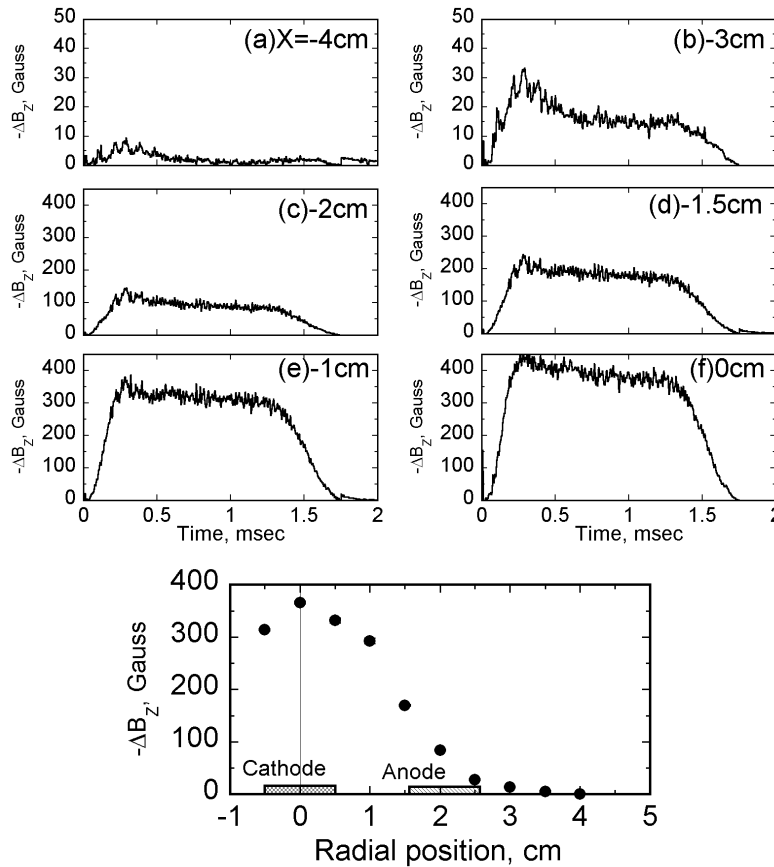
Figure 6. Time evolution and radial profiles of a diamagnetic signal. I_d =7.2 kA, helium mass flow rate dm/dt of 0.1g/s.

4

B. Evaluation of Lorentz force in the MPDT plasma

Figure 5 shows dependences of u_z, u_θ, T_i and M_i on discharge current I_d in a uniform applied-field of 870 G with helium mass flow rate dm/dt of 0.1g/s. Both of u_z and u_θ increase almost linearly with I_d, however, T_i increases steeply when I_d is more than 8 kA. Consequently, M_i saturates less than unity. In this case, an input electric energy converts into a thermal energy rather than a flow energy and undesirable ion heating occurred.

We measured spatial profiles of three components of the magnetic field in the plasma flow by the multi-channel magnetic probe array and evaluated the spatial distribution of Lorentz force field[8]. Time evolutions of the decrement of B_0, $-\Delta B_z$, are measured at $Z = 20$ cm as shown in Fig. 6(a)-(f). This decrement is caused by the diamagnetic effect of a high density MPDT plasma in a magnetic field. A radial profile of the diamagnetic variation of B_0 at $t = 1$ msec in a uniform applied-field of 870 G is also shown in Fig.6. A net field strength $B_z (= B_0 - \Delta B_z)$ decreases to about one half of the applied-field at the center of the plasma. An axial profile of the net strength of B_z is shown in Fig. 7(a). An azimuthal magnetic field B_θ is induced by the axial plasma current extending downstream along the plasma flow. The resultant magnetic flux tube converges gradually downstream, *i.e.* a slightly converging helical magnetic nozzle
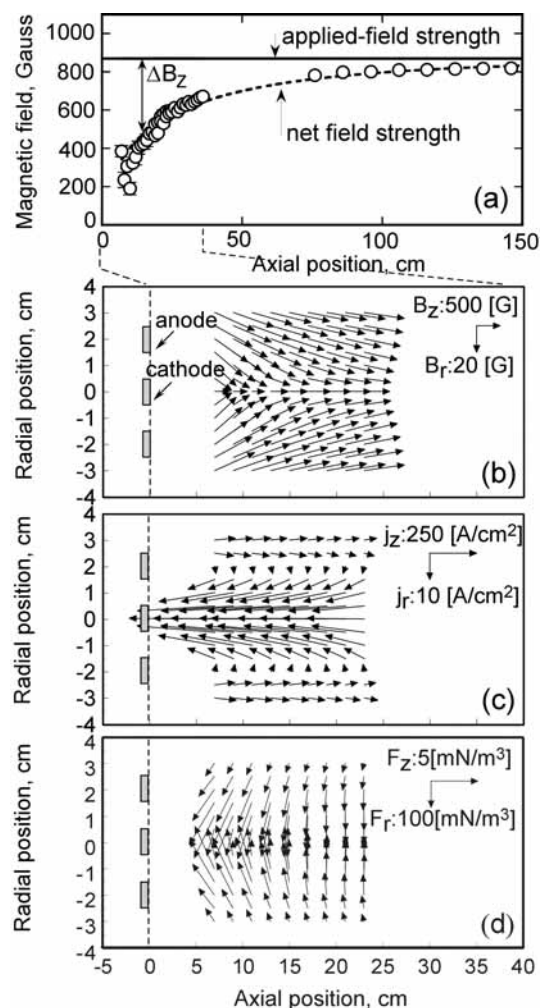
Figure 7. (a)Axial profiles of an externally-applied uniform magnetic field and net magnetic field strength. 2-D vector plots of (b)magnetic field, (c)plasma current density and (d)Lorentz force in the uniform applied-field.
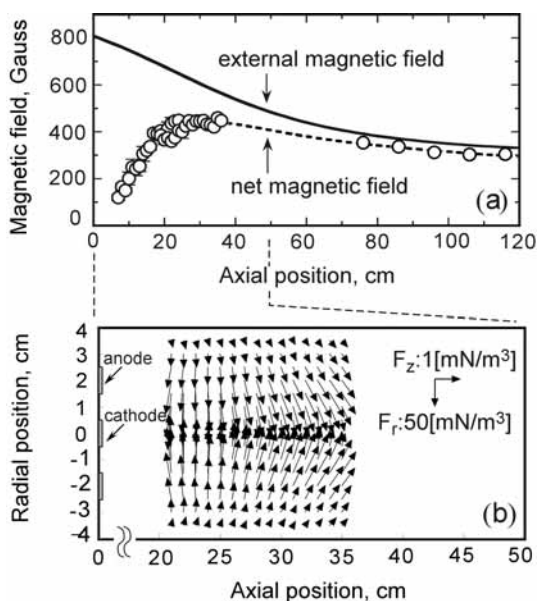
Figure 8. (a) Axial profiles of an externally-applied diverging magnetic field and net magnetic field strength. (b) 2-D vector plots of Lorentz force in the diverging applied-field.

with a variable pitch is spontaneously formed.

Plasma current density is calculated by Maxwell equation under the assumption of axisymmetry. Figure 7(b), (c) and (d) show two-dimensional (2-D) vector plots of radial-axial component of magnetic fields B_r and B_z, plasma current densities j_r and j_z and Lorentz force fields F_r and F_z, respectively. It should be noted that the inward radial component of the Lorentz force F_r (pinch force) is much larger than the axial component F_z in the measured region. Here F_z is calculated as $F_z = j_r B_\theta - j_\theta B_r$. The second term, $-j_\theta B_r$, comes from the interaction between j_θ due to diamagnetic current and Hall current and B_r generated in the resultant converging magnetic field. This term acts as a deceleration force canceling the acceleration force of the first term ($j_r B_\theta$). These results are consistent with the experimental results that M_i is always below unity in case of a uniform applied magnetic field[6].

In order to realize more efficient plasma acceleration, the sign of B_r of the ($-j_\theta B_r$) term should be reversed by externally applying a diverging magnetic field. Figure 8(a) shows an externally-applied diverging field and measured net field strength. Though a converging nozzle is still formed by the strong diamagnetic effect in the upstream region, it converts to a diverging field in the downstream region, where the diamagnetic effect decreases gradually; *i.e.*, a magnetic Laval nozzle is spontaneously formed. Spatial distribution of the Lorentz forces in the externally-applied diverging magnetic field is shown in Fig. 8(b). It is noteworthy that the direction of F_z converts from negative to positive in the region where the net magnetic flux tube changes from a converging one to a diverging one. This result shows that the Lorentz force distribution in the MPDT plasma can be controlled by adjusting the externally-applied field configuration. In addition to the conversion of the axial Lorentz force, a thermal energy of plasma is expected to be converted to an axial flow energy by passing through the magnetic Laval nozzle. Therefore, for more efficient plasma acceleration, the magnetic Laval-nozzle shape should be optimized by taking into account both an electromagnetic force and a plasma pressure gradient. This is a crucial ongoing task for a further progress in the plasma acceleration research[9].

IV.   Conclusion

The flow field and Lorentz force field in the applied-field MPDT plasma is measured experimentally. Considering the radial force balance of the plasma column, the plasma rotation phenomena are found to be a rigid body rotation as a result of several electromagnetic effects. Spatial distribution of Lorentz force field is evaluated from the magnetic field measurement. It is found that the high-beta plasma generated in the outlet of the MPDT diminishes the external magnetic field by the diamagnetic effect and a converging helical magnetic nozzle with a variable pitch is spontaneously formed. When a diverging magnetic field is applied externally, a magnetic Laval nozzle is spontaneously formed and the deceleration term changes its sign resulting in an increase of the acceleration force in the region of a diverging net magnetic field. For a more efficient plasma acceleration, the shape of an applied magnetic field should be optimized by taking both an electromagnetic force and a plasma pressure gradient into consideration.

References

[1]Jahn, R.G., *Physics of Electric Propulsion*, McGraw-Hill, New York, 1968.

[2]Sasoh, A. and Arakawa. Y., "Electromagnetic Effects in an Applied-Field Magnetoplasmadynamic Thruster," *Journal of Propulsion and Power*, Vol. 8, 1992, pp.98-102.

[3]Tahara, H., Kagaya, Y. and Yoshikawa, T., "Effects of Applied Fields on Performance of a Quasisteady Magnetoplasmadynamic Arcjet," *Journal of Propulsion and Power*, Vol. 11, 1995, pp.337-342.

[4]Tahara, H., Kagaya, Y. and Yoshikawa, T., "Performance and Acceleration Process of Quasisteady Magnetoplasmadynamic Arcjets with Applied Magnetic Fields," *Journal of Propulsion and Power*, Vol. 13, 1997, pp.651-658.

[5]Ando, A., Ashino, M., Sagi, Y., et al., "Spectroscopic Studies of High-Mach Number Rotating Plasma Flow," *Journal of Plasma Fusion Research SERIES*, Vol.4, 2001, pp.373-378.

[6]Inutake, M., Ando, A., et al., "Characteristics of a Supersonic Plasma Flow in a Magnetic Nozzle," *Journal of Plasma Fusion Research*, Vol.78, 2002, pp.1352-1360.

[7]Inutake, M., Ando, A., et al., "Magnetic-Nozzle Acceleration and Ion Heating of a Supersonic Plasma Flow," *Transactions of Fusion Science and Technology*, Vol.43, 2003, pp.118-124.

[8]Tobari, H., Inutake, M., Ando, A. and Hattori, K., "Spatial Distribution of Lorentz Forces in an Applied-Field Magneto-Plasma-Dynamic Arcjet Plasma," *Journal of Plasma Fusion Research*, Vol.80, 2004, pp.651-652.

[9]Inutake, M., Ando, A., et al., presented in this conference.